Collocation Discrete Least Square (CDLS) Method for Elasticity Problems

Mohammad Naisipour[1], Mohammad Hadi Afshar[2,*], Behrooz Hassani[3], Ali Rahmani Firoozjaee[4]

Received:June 2007, revised:June 2008, accepted: January 2009

Abstract: *A meshless approach, collocation discrete least square (CDLS) method, is extended in this paper, for solving elasticity problems. In the present CDLS method, the problem domain is discretized by distributed field nodes. The field nodes are used to construct the trial functions. The moving least-squares interpolant is employed to construct the trial functions. Some collocation points that are independent of the field nodes are used to form the total residuals of the problem. The least-squares technique is used to obtain the solution of the problem by minimizing the summation of the residuals for the collocation points. The final stiffness matrix is symmetric and therefore can be solved via efficient solvers. The boundary conditions are easily enforced by the penalty method. The present method does not require any mesh so it is a truly meshless method. Numerical examples are studied in detail, which show that the present method is stable and possesses good accuracy, high convergence rate and high efficiency.*

Keywords: *Meshless method, MLS, Least square technique, CDLS, Elasticity*

1. Introduction

In the recent decade, a new class of numerical methods, meshless methods (also called mesh-free methods), have been developing fast [1, 2]. These methods have become an important tool in computational solid mechanics, owing to their advantages over the traditional finite element method (FEM), finite-volume method (FVM), and finite-difference method (FDM). Meshless methods rely only on a group of scatter points, which means not only that the burdensome work of mesh generation is avoided, but also more accurate description of irregular complex geometries can be achieved. Furthermore, the meshless approximation has higher smoothness, and no additional post-processing is needed.

In the field of meshless methods for solving elasticity problems, Krysl and Belytschko [3] employed Element-Free Galerkin Method (EFGM) to analyze thin plates; Onate et al. [4] proposed a stabilization technique by introducing new terms in both the governing equations and the traction boundary conditions to solve elasticity problems; Kwon et al. [5] presented a least-squares meshfree method for solving linear elastic problems; Zhang et al. [6] proposed a meshless weighted least-squares (MWLS) method, to solve problems of elastostatics; Atluri et al. proposed a MLPG mixed collocation method [7] and MLPG mixed finite difference method [8] for solid mechanics.

All the above meshless methods can be categorized into two groups according to their discretization scheme. The first group is Galerkin-based meshless methods (GBMMs), of which the EFGM proposed by Belytschko in 1994 [9] is a famous representative. In GBMMs, the highest order of derivatives is lowered by using a weak form of the original partial differential equations (PDEs). The accuracy of GBMMs is high, and good stability can always be obtained. The main shortcoming of GBMMs is that the integrals in the weak form must be evaluated properly. One way of evaluating integrals is to use a background mesh, which makes the method not truly meshless; another is to use nodal integration [10], which results in significant errors because the divergence theorem used in the establishment of the weak form demands accurate integration [11]. In addition, because meshless shape functions are too complex to be expressed in closed form, a delicate background mesh and a large number of

* *Corresponding author: Email:mhafshar@iust.ac.ir*

1 *M.Sc. Student, Civil Engineering Dept., Iran university of science and technology, Tehran, Iran m_naisipour@civil.iust.ac.ir*

2 *Associate Professor, Civil Engineering Dept., Iran university of science and technology, Tehran, Iran.mhafshar@iust.ac.ir*

3 *Associate Professor, Civil Engineering Dept., Shahrood university of technology, Shahrood, Iran b_hassani@yahoo.com*

4 *M.Sc. of Civil Engineering, Hydraulic Structures, Sahid bahonar university, Kerman, Iran ar_firoozjaee@ yahoo.com*

quadrature points are always employed, which decreases the efficiency seriously. As a consequence, GBMMs are much more computationally expensive than the FEM.

The other group of meshless methods is built on collocation schemes. The SPH, FPM, DAM, least-square collocation meshless method [12], point weighted least-square (PWLS) method [13], and radial basis function (RBF) collocation methods [14–17] all belong to this group. These methods are very efficient and easy to program, but they usually suffer from poor stability, and the accuracy often goes down near the boundary.

The universal law of least squares can also be used for discretization. In fact, it has been introduced into the FEM successfully [18]. A truly meshless method based on the least-squares approach, the collocation discrete least-squares (CDLS) method, was proposed to solve Poisson's equation [19] and free surface seepage problem [20] and also was presented for error estimation and adaptive refinement [21]. In this paper CDLS method, already used for the solution of hyperbolic problems, is extended for solving elasticity problems. In the present CDLS method, the problem domain is discretized by distributed field nodes. The field nodes are used to construct the trial functions by employing the moving least-squares interpolant. Some collocation points that are independent of the field nodes are used to form the total residuals of the problem. The least-squares technique is used to obtain the solution of the problem by minimizing the summation of the residuals for the collocation points. Because of using the least-squares technique and more collocation points the CDLS method is not bothered by instability as collocation-based meshless methods.

In this article, the CDLS method is extended to solve elasticity problems. Constructing of moving least square shape functions is explained in Section 2; discretization of equilibrium equations in solid mechanics using collocation discrete least square (CDLS) method is described in Section 3; numerical examples are demonstrated in Section 4; and some concluding remarks are presented in Section 5.

2. Moving least square shape functions

Among the available meshless approximation schemes, the moving least squares (MLS) method [22] is generally considered to be one of the best methods to interpolate random data with a reasonable accuracy, because of its completeness, robustness and continuity[7, 23]. With the MLS interpolation, the unknown function Φ is approximated by:

$$\Phi(x) = \sum_{i=1}^{m} P_i(x) a_i(x) = P^T(x) a(x) \tag{1}$$

Where $P^T(x)$ is a polynomial basis in the space coordinates, and m is the total number of the terms in the basis. For a 2D problem we can specify $P = [1 \;\; x \;\; y \;\; x^2 \;\; xy \;\; y^2]$ for $m=6$. $a(x)$ is the vector of coefficients and can be obtained by minimizing a weighted discrete L_2 norm as follows:

$$J = \sum_{i=1}^{n} w_j(x-x_j)\left(P^T(x_j)a(x) - u_j^h\right)^2 \tag{2}$$

The weight function $w_j(x-x_j)$ is usually built in such a way that it takes a unit value in the vicinity of the point j where the function and its derivatives are to be computed and vanishes outside a region Ω_j surrounding the point x_j. In this research the cubic spline weight function is considered as follows:

$$w(x-x_j) = w(\bar{d}) = \begin{cases} \frac{2}{3} - 4\bar{d}^2 + 4\bar{d}^3 & for \quad \bar{d} \le \frac{1}{2} \\ \frac{4}{3} - 4\bar{d} + 4\bar{d}^2 - \frac{4}{3}\bar{d}^3 & for \quad \frac{1}{2} < \bar{d} \le 1 \\ 0 & for \quad \bar{d} > 1 \end{cases} \tag{3}$$

Where $\bar{d} = \|x - x_j\| / d_w$ and d_w is the size of influence domain of point x_j.

Minimization of equation (2) leads to

$$\Phi(x) = P^T(x) A^{-1}(x) B(x) \Phi^h \tag{4}$$

where

$$A(x) = \sum_{j=1}^{n} w_j(x-x_j)\; P(x_j)\; P^T(x_j) \tag{5}$$

$$B(x) = [w_1(x-x_j)P(x_1),\; w_2(x-x_2)P(x_2),\ldots,\; w_n(x-x_n)P(x_n)] \tag{6}$$

Comparing equation (4) with the well known

form of equation (7) yields to equation (8)

$$\Phi(x) = N^T(x)\Phi^h \tag{7}$$

$$N^T(x) = P^T(x)A^{-1}(x)B(x) \tag{8}$$

$N^T(x)$ Contains the shape functions of nodes at point (X) witch are called moving least square (MLS) shape functions.

3. Collocation Discrete least square (CDLS) method

Consider the following (partial) differential equation

$$A(\Phi) + f = 0 \qquad in\ \Omega \tag{9}$$

subject to appropriate Drichlet and Neumann boundaries.

$$\Phi - \overline{\Phi} = 0 \qquad on \quad \Gamma_u \tag{10}$$

$$B(\Phi) - \bar{t} = 0 \qquad on \quad \Gamma_t \tag{11}$$

Where A and B are (partial) differential operators, and f represents external forces or source term on the problem domain.

Upon discretization of the problem domain and its boundaries using Equation (7) defined as the residual of partial differential equation at a typical collocation point k is:

$$R_\Omega(x_k) = A(\Phi(x_k)) + f(x_k) = \sum_{j=1}^{n} A(N_j(x_k))\Phi_j + f(x_k) \qquad k = 1 \approx M \tag{12}$$

the residual of Neumann boundary condition at typical collocation k on the Neumann boundary can also be written as:

$$R_t(x_k) = B(\Phi(x_k)) - \bar{t}(x_k) = \sum_{j=1}^{n} B(N_j(x_k))\Phi_j - \bar{t}(x_k) \qquad k = 1 \approx M_t \tag{13}$$

and finally the residual of Drichlet boundary condition at nodes on the Drichlet boundary could be stated by:

$$R_u(x_k) = \Phi - \overline{\Phi}(x_k) = \sum_{j=1}^{n} N_j(x_k)\Phi_j - \overline{\Phi}(x_k) \qquad k = 1 \approx M_u \tag{14}$$

where n is the total number of nodes, M_Ω is the internal collocation points, M_t is the collocation points on the Neumann boundary, M_u is the collocation points on the Dirichlet boundary and M is the total number of collocation points. A penalty approach is used to form the total residual of the problem defined as:

$$I = \sum_{k=1}^{M} (R_\Omega{}^2(x_k)) + a_t \sum_{k=1}^{M_t} (R_t{}^2(x_k)) + a_u \sum_{k=1}^{M_u} (R_u{}^2(x_k)) \tag{15}$$

$$I = \sum_{k=1}^{M}\sum_{j=1}^{n} [\ A(N_j(x_k)\Phi_j + f(x_k)]^2 + a_t \sum_{k=1}^{M_t}\sum_{j=1}^{n} [\ B(N_j(x_k)\Phi_j + \bar{t}(x_k)]^2 + a_u \sum_{k=1}^{M_u}\sum_{j=1}^{n} [\ (N_j(x_k)\Phi_j + \overline{\Phi}(x_k)]^2 \tag{16}$$

Where a_t and a_u are penalty coefficients for Neumann and Drichlet boundary conditions respectively. To impose the boundary conditions exactly, the penalty factor must be infinite, which is not possible in practical numerical analysis [24]. Therefore, in the penalty method boundary conditions can not be satisfied exactly, but only approximately. In general, the use of a larger penalty factor will lead to better enforcement of the constraint. On the other hand, if the penalty factor is too small, the constraints will not be properly enforced, but if it is too large, numerical problems will be encountered. A compromise should, therefore, be reached. Penalty coefficients set to be 10^8 in this research.

Minimization of the functional with respect to nodal parameters $(\Phi_i, i = 1,2,...,n)$ leads to the following system of equations.

$$K\Phi = F \tag{17}$$

where

$$K_{ij} = \sum_{k=1}^{M} A(N_j(x_k))A(N_j(x_k)) + a_t \sum_{k=1}^{M_t} B(N_j(x_k))B(N_j(x_k)) + a_u \sum_{k=1}^{M} N_j(x_k)N_j(x_k) \tag{18}$$

$$F_i = \sum_{k=1}^{M} A(N_j(x_k))f(x_k) + a_t \sum_{k=1}^{M_t} B(N_j(x_k))\bar{t}(x_k) + a_u \sum_{k=1}^{M} N_j(x_k)\overline{\Phi}(x_k) \tag{19}$$

the stiffness matrix K in Eq. (17) is square (NxN) and symmetric. Therefore, the final system of equations can be solved directly via efficient solvers.

4. Numerical examples

In this section, some 2D numerical examples, which are solved by the CDLS method, are presented. The examples include: 1) the patch test, 2) a cantilever beam under end point load, and 3) an infinite plate with a circular hole under uniaxial load. Problems 2 and 3 are solved using regular nodal distributions. For information about the influence of the irregular nodal configuration on the CDLS performance see [26].

4.1 The Patch Test

The standard patch test: a rectangle under uniform tension load (see Fig. 1) is solved as the first example. The material parameters are as follows: the Young's modulus $\boldsymbol{E}$ = 1000.0, and the Poisson's ratio $\boldsymbol{\nu}$ = 0.3. Plane stress condition is assumed for the 2D problem and 9 nodes are used. Two nodal configurations are used for the testing: one is regular, and another is irregular, as shown in Fig.1. The proper displacement constraints are applied to the bottom edge.

The simulation results show a linear displacement on the lateral edges, and constant displacement on the top edge; the normal stress in the loading direction is constant and there is no shear stress in the solution domain.

4.2 Cantilever Beam

In the second example, we solve a cantilever beam under a point load at the end, as shown in Fig.2. For this problem, the exact stress and displacement solution for plane stress is given in Timoshenko and Goodier [25] as

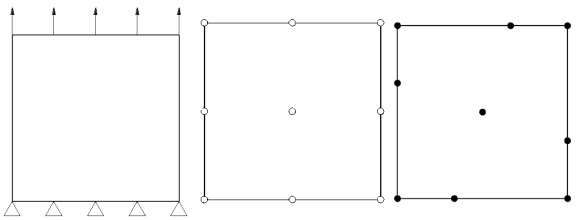

Figure 1 The patch test: a rectangle under uniform tension. The two nodal configurations

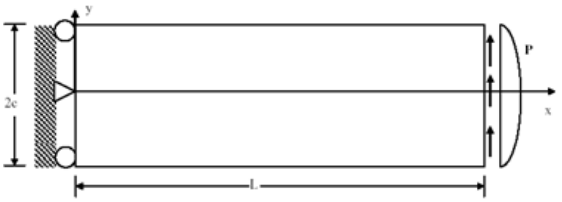

Figure 2 A cantilever beam under a point load at the end

$$\sigma_x = -\frac{P(L-x)y}{I}$$
$$\sigma_y = 0 \qquad (20)$$
$$\tau_{xy} = \frac{P}{2I}[c^2 - y^2]$$

and

$$u = -\frac{Py}{6EI}[3x(2L-x) + (2+\nu)(y^2 - c^2)]$$
$$v = \frac{Py}{6EI}[x^2(3L-x) + 3\nu(L-x)y^2 + (4+5\nu)c^2 x] \qquad (21)$$

where the moment of inertia $I = 2c^3/3$ for a beam with rectangular cross-section and unit thickness. The problem is solved using the CDLS method under plane stress condition with the following constants: $\boldsymbol{P}$ = 1, $\boldsymbol{E}$ = 1000, $\boldsymbol{c}$ = 2, $\boldsymbol{L}$ = 24, and $\boldsymbol{\nu}$ = 0.3.

Regular uniform nodal configurations with nodal distances, $\boldsymbol{d}$, of 1.0, 0.5, and 0.25 are used. The corresponding numbers of nodes are 125, 441, and 1649, respectively. and the corresponding numbers of collocation points are 221, 825, and 3185, respectively. The nodal configurations are shown in Fig.3. This problem is simulated using the MLS with the second order polynomial basis. Fig.4 shows the vertical displacement along the central line of the beam for the nodal configuration with $\boldsymbol{d}$ = 1.0. The simulation prediction agrees with the analytical solution very well. Fig.5 shows the shear stress distribution of cantilever beam at $\boldsymbol{x=L/2}$ for the three nodal configurations with $\boldsymbol{d}$ = 1.0, $\boldsymbol{d}$ = 0.5 and $\boldsymbol{d}$ = 0.25 and a very good agreement with the analytical solution is obtained. The Contours of σ_x stress and the vertical displacement for the nodal configuration with $\boldsymbol{d}$ = 0.25 are shown in

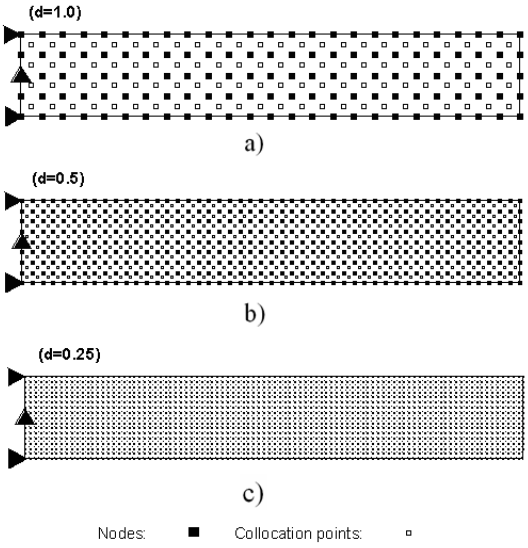

Figure 3 The nodal configuration of the cantilever beam, a) 125 nodes and 221 collocation points b) 441 nodes and 825 collocation points c) 1649 nodes and 3185 collocation points

Fig.6 and 7 respectively. The convergence rate is studied with three nodal configurations (d =1.0, 0.5, and 0.25). The following H1 error norm are used for showing the convergence rate in Fig.8.

$$\|e\|_{H^1}^2 = \sum_{i=1}^{N} \left[\begin{array}{l} (u-u^h)_i^2 + (v-v^h)_i^2 + (\sigma_x - \sigma_x{}^h)_i^2 + \\ (\tau_{xy} - \tau_{xy}{}^h)_i^2 + (\sigma_x - \sigma_y{}^h)_i^2 \end{array} \right] \qquad (22)$$

Where N is number of nodes. The results clearly show that a stable convergence rate is obtained for the present CDLS method.

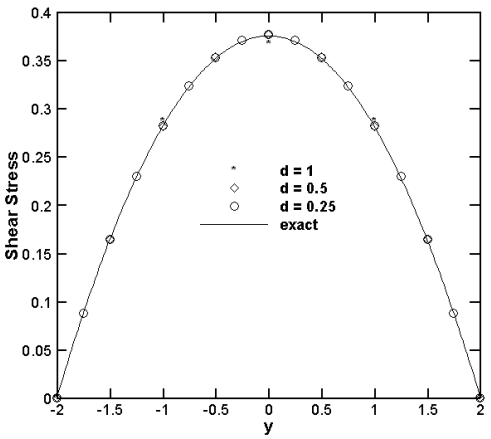

Figure 5 The shear stress distribution of cantilever beam at x=L/2

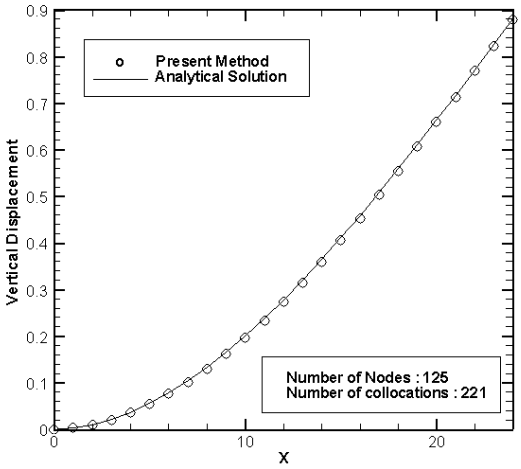

Figure 4 The vertical displacement of the cantilever beam under the end load

4.3 Infinite Plate with a Circular Hole

Finally, we show the computational results of an infinite plate with a circular hole subjected to a uniaxial traction P at infinity as shown in Fig.9. The exact solutions for stresses and displacements for this problem are

$$\begin{aligned} \sigma_x &= P\left\{1 - \frac{a^2}{r^2}\left[\frac{3}{2}\cos(2\theta) + \cos(4\theta)\right] + \frac{3a^4}{2r^4}\cos(4\theta)\right\} \\ \sigma_y &= -P\left\{\frac{a^2}{r^2}\left[\frac{1}{2}\cos(2\theta) - \cos(4\theta)\right] + \frac{3a^4}{2r^4}\cos(4\theta)\right\} \\ {}_{xy} &= -P\left\{\frac{a^2}{r^2}\left[\frac{1}{2}\sin(2\theta) + \sin(4\theta)\right] - \frac{3a^4}{2r^4}\sin(4\theta)\right\} \end{aligned} \qquad (23)$$

and

$$\begin{aligned} u_r &= \frac{P}{4G}\left\{\begin{array}{l} r\left[\frac{k-1}{2} + \cos(2\theta)\right] + \\ \frac{a^2}{r}\left[1 + (1+k)\cos(2\theta)\right] - \\ \frac{a^4}{r^3}\cos(2\theta) \end{array}\right\} \\ u_\theta &= \frac{P}{4G}\left\{(1-k)\frac{a^2}{r} - r - \frac{a^4}{r^3}\right\}\sin(2\theta) \end{aligned} \qquad (24)$$

respectively. In the above equations, G is the shear modulus and $k=(3-\nu)/(1+\nu)$ with ν the Poisson's ratio. Due to symmetry, only the upper right square quadrant of the plate is modeled [see Fig. 9]. The edge length of the square is $5a$, with

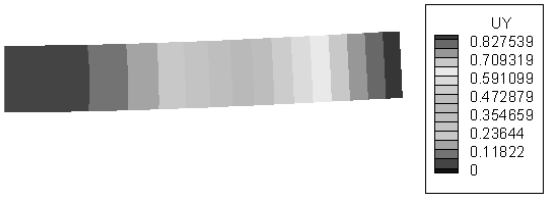

Figure 6 Contours of vertical displacement (Regular grid of 1649 nodes)

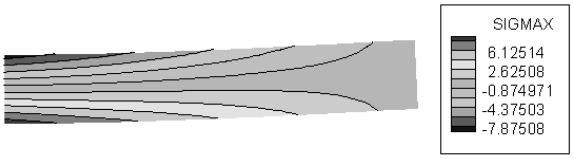

Figure 7 Contours of σ_x stress (Regular grid of 1649 nodes)

a being the radius of the circular hole. Symmetry boundary conditions are imposed on the left and bottom edges and the tractions obtained from the analytical solution [Eq. 23] are applied to the top and right edges.

The problem is solved using the CDLS method, under a plane stress condition, with the following constants: P =1, E = 1000, and v=0.3. Three nodal configurations with 183, 318 and 633 nodes, respectively, are used. The nodal configurations are shown in Figure 10. The MLS with quadratic basis is used in the simulation. The horizontal displacement $\boldsymbol{u_x}$ along the bottom edge (y = 0), and the stress component σ_x along the left edge (x = 0) are shown in Figure 11 and Figure 12, respectively. Compared with the analytical solutions, good agreements are obtained for both the displacements and stresses.

Fig.13 shows convergence rate with three nodal configurations (n =183, 318, and 633). The following L2 norm of error is used for representing the convergence rate of displacements and stress separately:

$$\|e\|_{L^2}^2 = \sum_{i=1}^{N} e_i^2 \qquad (25)$$

Where $\boldsymbol{e_i}$ is the difference between numerical

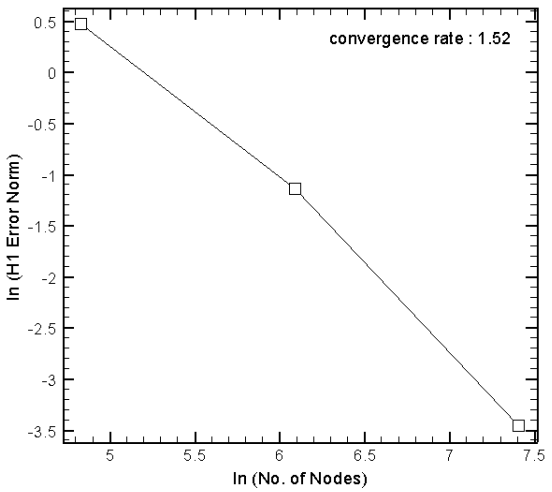

Figure 8 The convergence rate in the cantilever beam under the end load

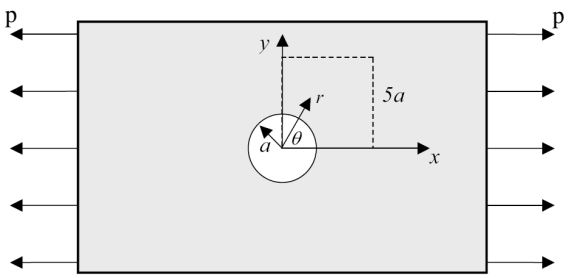

Figure 9 An infinite plate with a circular hole under a uniaxial load

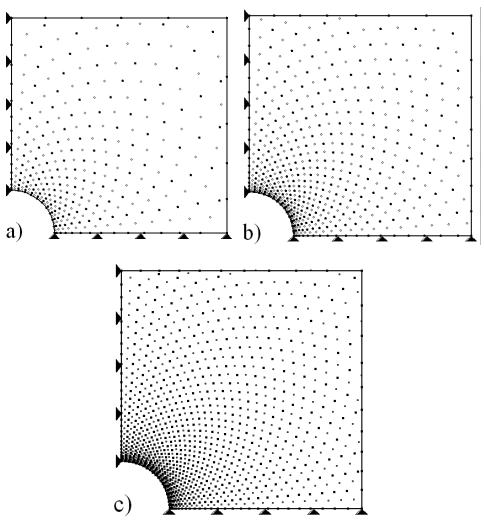

Figure 10 The nodal configurations of the infinite plate with a circular hole
a) 183 nodes and 335 collocation points b) 318 nodes and 598 collocation points c) 633 nodes and 1215 collocation points

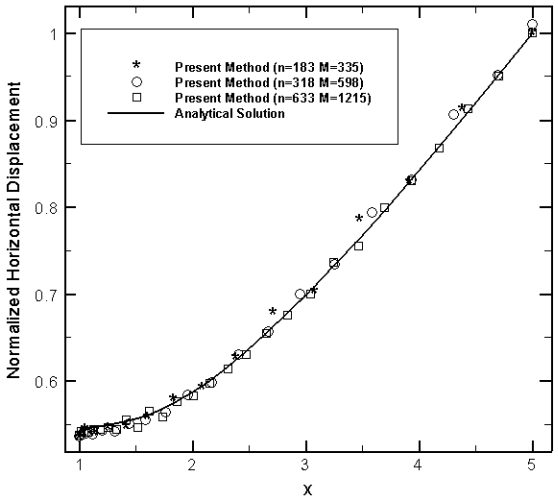

Figure 11 The horizontal displacement along y=0 for the three nodal configurations

and exact solution in node i. A stable and monotonic convergence rate is observed for the problem.

This problem is also solved for the special case where the collocation points are placed on the position of main nodes. Distribution of nodes with 183 nodes and collocations is shown in Figure 14. For this case H^1 error norm [Eq. 22] is 1.11. By increasing number of collocations to 335 (see Figure 10-a), H^1 norm decreases to 0.79. For additional information about effect of collocation points refer to [26].

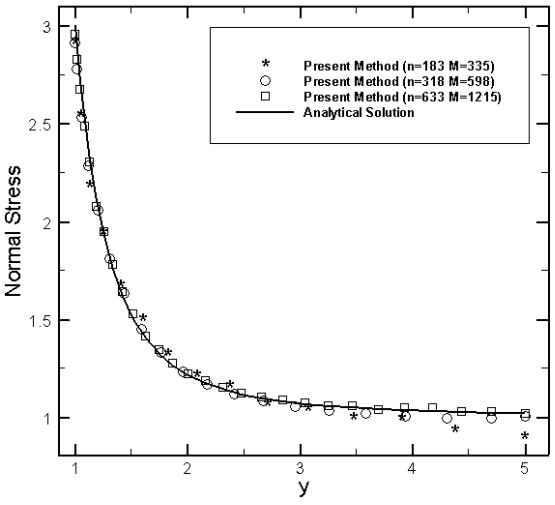

Figure 12 The normal stress σ_x along x = 0 for the three nodal configurations

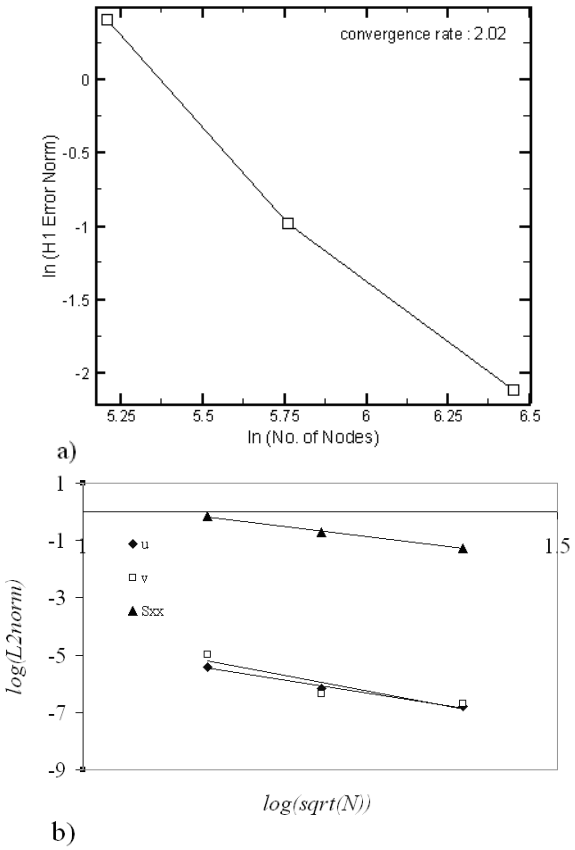

Figure 13 The convergence rate of the infinite plate with a circular hole. a) H^1 error norm and b) L^2 error norm of displacements and normal stress

Finally, the CDLS method is compared with FPM. FPM results are taken from [4]. Nodal configurations for CDLS and FPM are shown in Figure 15 and 16, respectively. The exact stress component σ_x along the left edge (x = 0) is compared with corresponding results from both CDLS and FPM in Figure 17. Results shows that present method possesses good accuracy in comparison with FPM method.

5. Conclusion

A truly meshless approach, collocation discrete least-squares (CDLS) method, is extended to solve elasticity problems. In the CDLS method, the problem domain is discretized by distributed field nodes. The field nodes are used to construct the trial functions. The moving least-squares interpolant is employed to construct

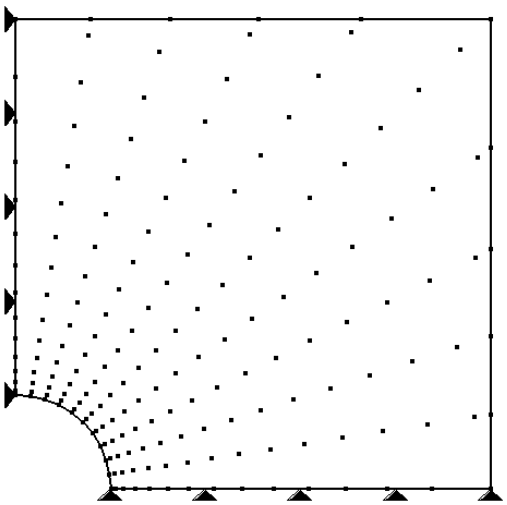

Figure 14 The nodal configuration of the infinite plate with a circular hole of 183 nodes and 183 collocation points

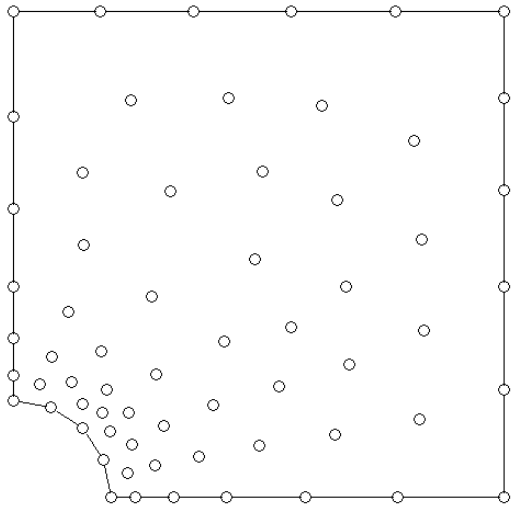

Figure 15 The nodal configuration of the infinite plate with a circular hole of 64 nodes and collocation points for CDLS solution

the trial functions. Some collocation points that are independent of the field nodes are used to form the total residuals of the problem. The least-squares technique is used to obtain the solution of the problem by minimizing the summation of the residuals for the collocation points. The final coefficient matrix is symmetric and then can be solved directly via efficient solvers. The boundary conditions are easily enforced by penalty method. The present CDLS method does not require any mesh so it is a truly meshless method. Numerical examples are studied in detail, which show that the present method is stable and possesses good accuracy, high convergence rate and high efficiency. It is also shown that CDLS method has good accuracy in comparison with FPM method. All these advantages of the CDLS emphasizes on its ability as a useful meshless method for the solution of elasticity problems.

References

[1] Belytschko, T., Krongauz, Y., Organ D., Fleming M., and Krysl P.: 1996, Meshless methods: an overview and recent developments, Comput. Meth. Appl. Mech. Eng.139, 3–47.

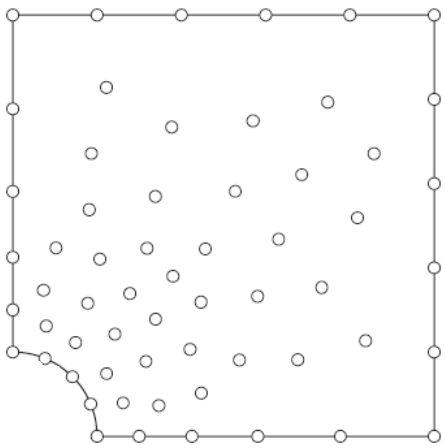

Figure 16 The nodal configuration of the infinite plate with a circular hole of 60 points for FPM solution

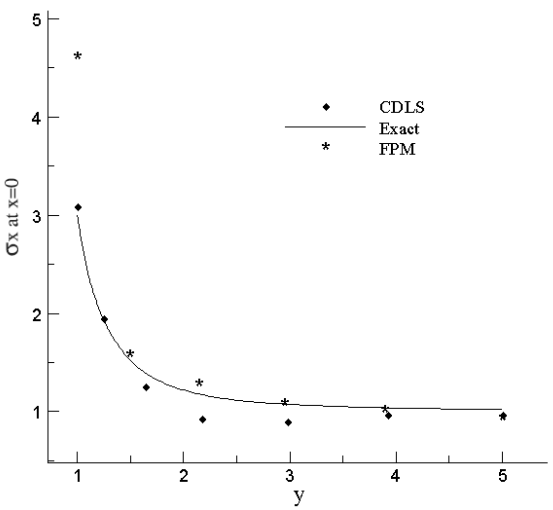

Figure 17 The normal stress σ_x along x = 0

[2] Li, S., Liu, W. K.: 2002, Meshfree and particle methods and their applications, Appl. Mech. Rev.55, 1–34.

[3] Belytschko T, Krysl P.: 1995, Analysis of thin plates by the element-free Galerkin method, Computational Mechanics.17, 26-35.

[4] Onate E., Perazzo, F., Miquel, J.: 2001, A finite point method for elasticity problems, Computers and Structuresl.79, 2151-2163.

[5] Kwon, K.C., Park, S.H., Jiang, B.N., and Youn, S.K.: 2003, The least-squares meshfree method for solving linear elastic problems, Computational Mechanics.30, 196-211.

[6] Zhang X., Pan, X. F., Hu, W., and Lu, M. W.: 2002, Meshless weighted least-square method, Fifth World Congress on Computational Mechanics, Vienna, Austria.

[7] Atluri, S. N., Liu, H. T., Han, Z. D.: 2006, Meshless Local Petrov-Galerkin (MLPG) mixed collocation method for elasticity problems, CMES: Computer Modeling in Engineering & Sciences.14, 141-152.

[8] Atluri, S. N., Liu, H. T., Han, Z. D.: 2006, Meshless Local Petrov-Galerkin (MLPG) mixed finite difference method for solid mechanics, CMES: Computer Modeling in Engineering & Sciences.15, 1-16.

[9] Belytschko, T., Lu, Y. Y., and Gu, L.: 1994, Element Free Galerkin Method, Int. J. Numer. Meth. Eng.37, 229–256.

[10] Beissel, S., and Belytschko, T.: 1996, Nodal integration of the element-free Galerkin method, Comput. Meth. Appl. Mech. Eng.139, 49–74.

[11] Park, S. H., and Youn, S. K.: 2001, The least-square meshfree method, Int. J. Numer. Meth. Eng.52, 997–1012.

[12] Zhang, X., Liu, X.-H., Song, K.-Z., and Lu, M.-W.: 2001, Least-square collocation meshless method, Int. J. Number. Meth. Eng.51, 1089–1100.

[13] Wang, Q.X., Li, H., Lam, K.Y.: 2005, Development of a new meshless – point weighted least–squares (PWLS) method for computational mechanics. Computational Mechanics.35, 170 –181.

[14] Chen, J. T., Chang, M. H., and Chen, K. H., Chen, I. L.: 2002, Boundary collocation method for acoustic eigenanalysis of three-dimensional cavities using radial basis function, Comput. Mech.29, 392–408.

[15] Chen, W.: 2002, Symmetric boundary knot method, Eng. Anal. Bound. Elem.26, 489–494.

[16] Chen, W., and Hon, Y. C.: 2003, Numerical convergence of boundary knot method in the analysis of helmholtz, modified helmholtz, and convection-diffusion problems, Comput. Meth. Appl. Mech. Eng.192, 1859–187.

[17] Zhang, X., Song, K.-Z., and Lu, M.-W.:2000, Meshless methods based on collocation with radial basis functions, Comput. Mech.26, 333–343.

[18] Jiang, B. N.: 1998, The least-squares finite element method: theory and applications in computational fluid dynamics and electromagnetics, chap. 1, Springer-Verlag, Berlin.

[19] Arzani1, H., and Afshar, M. H.: 2006, Solving Poisson's equations by the discrete least square meshless method, WIT Transactions on Modelling and Simulation.42, 23–31.

[20] Firoozjaee, A. R., and Afshar, M. H.: 2007, Collocation discrete least square meshless method for the solution of free surface seepage problem, International Journal of

Civil Engineering, 5(2): 134-143.

[21] Lashckarbolok, M., and Afshar, M. H.: 2007, Collocated discrete least square (CDLS) meshless method: error estimate and adaptive refinement, Int. J. Numer. Meth. Fluids, In press.

[22] Lancaster, P., and Salkauskas, K.: 1981, Surfaces generated by moving least squares method. Mathematics of computation.37, 141-158.

[23] Atluri, S. N.:2004, The Meshless Local Petrov-Galerkin (MLPG) method for domain & boundary discretizations, Tech Science Press.

[24] Liu, G. R.,: 2003, Mesh free methods: moving beyond the finite element method, CRC Press.

[25] Timoshenko, S.P., and Goodier, J.N.: 1987, Theory of elasticity, 3rd edition, McGraw-Hill, New York.

[26] Firoozjaee, A. R., and Afshar, M. H.: 2008, Discrete least squares meshless method with sampling points for the solution of elliptic partial differential equations, Engineering Analysis with Boundary Elements, doi:10.1016/j.enganabound.2008.03.04.